Developing a fishery-independent index of relative abundance for Gulf of Mexico Pink Shrimp using VAST

Lisa Ailloud, Molly Stevens, Brendan Turley, Adam Pollack, and David Hanisko

SEDAR87-AP-04

31 January 2025

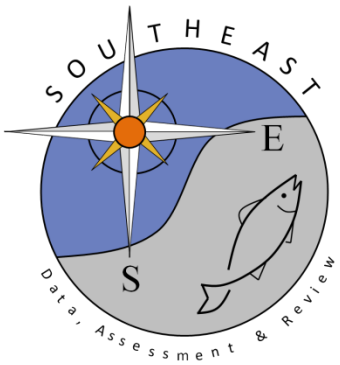

Please cite this document as:

Ailloud, Lisa, Molly Stevens, Brendan Turley, Adam Pollack, and David Hanisko. 2025. Developing a fishery-independent index of relative abundance for Gulf of Mexico Pink Shrimp using VAST. SEDAR87-AP-04. SEDAR, North Charleston, SC. 25 pp.

Developing a fishery-independent index of relative abundance for Gulf of Mexico Pink Shrimp using VAST.

Lisa Ailloud[1], Molly Stevens[2], Brendan Turley[3], Adam Pollack[4], and David Hanisko[4]
[1]*Southeast Fisheries Science Center (SEFSC), National Marine Fisheries Service (NMFS), National Oceanographic and Atmospheric Administration (NOAA), Charleston SC, USA*
[2]*SEFSC, NMFS, NOAA, St. Petersburg FL, USA*
[3]*Cooperative Institute of Marine and Atmospheric Studies; University of Miami, Miami, FL*
[4]*SEFSC, NMFS, NOAA, Pascagoula, MS, USA*

1. Introduction

Pink shrimp (*Farfantepenaeus duorarum*) indices of relative abundance were developed for consideration in the SEDAR 87 Gulf of Mexico (GOM) white, pink, and brown shrimp stock assessment process for input into JABBA, a Bayesian state-space surplus production modelling tool (Winker, Carvalho, and Kapur 2018).

Shrimp indices of abundance have historically been developed using standard delta-lognormal GLM approaches applied to data from the Southeast Area Monitoring and Assessment Program (SEAMAP) Groundfish Surveys (1987-present). For pink shrimp, the bulk of the stock is located in the Eastern GOM, for which data are available starting in 2008/09, after the SEAMAP survey expansion into Florida waters. Though the survey began operating in the East in the Fall of 2008, sampling south of Tampa was limited for the first couple of years (SEDAR 2023). The survey was only fully implemented to include all areas from Mobile Bay, AL to Key West, FL starting in 2010. In addition, the coverage of the SEAMAP Fall Survey was incomplete between 2008-2013 so Summer survey data has typically been used to develop the index of relative abundance for the stock. However, we were interested in combining the two datasets (Summer and Fall) in a single analysis for SEDAR 87, using an approach capable of taking into account the spatiotemporal gaps and shifts in survey coverage.

To that end, we used the Vector Autoregressive Spatio-Temporal (VAST) modeling platform to develop a single, continuous standardized index of abundance for pink shrimp. VAST is an R package for implementing a spatial delta-generalized linear mixed model (delta-GLMM) when standardizing survey data. It allows for predicting population density based on both habitat covariates (i.e., covariates that affect population density) and spatial and spatiotemporal random effects. This flexible framework capable of accounting for changes in the spatiotemporal footprint of surveys through time. For pink shrimp, the SEAMAP surveys (Summer and Fall) were used for developing a single, joint index of relative abundance for the stock. Since many studies point to the fact that environmental conditions (e.g., salinity and temperature) in the nursery grounds play an important role in driving the abundance and distribution of shrimp each year, we further explored whether the inclusion of environmental covariates could help explain the variability observed in the index through the used of habitat covariates in VAST.

This paper details the data, workflow, and results of applying the VAST modeling approach to Gulf of Mexico pink shrimp data to produce an index of relative abundance for the stock.

2. Methods

2.1 Stock description

Pink shrimp in the GOM range from the Florida Keys along the Gulf Coast to to the Yucatan south of Cabo Catoche, Mexico (SEDAR 2024a). Adults spawn offshore, year round, and their larvae settle into nearshore estuarine or marsh nursery habitat where they develop into juveniles and subadults before returning offshore. Pink shrimp have a short life span of less than 2 years, and have a distinctive behavior of burrowing during the day and emerging in the water column at night (*Figure 1*), which is typically when the fishery operates (SEDAR 2024a). The bulk of the US Gulf of Mexico pink shrimp catches occur in the Tortugas fishing grounds (Williams et al. 2024).

2.2 Data

2.2.1 Fishery Independent Surveys

A number of fishery-independent survey data time series were made available for SEDAR 87, and vetted during the Data Workshop (see Data Workshop Report (SEDAR 2024b) for more detail). The only data source that was retained for developing the index of relative abundance for the stock was the SEAMAP Groundfish survey. Data from the Florida Fish and Wildlife Conservation Commission's (FWC) Fisheries-Independent Monitoring (FIM) surveys were initially considered but ultimately dropped as they could not be easily combined with the SEAMAP data since there was no spatial overlap between the two surveys. SEAMAP data was favored over FWC data for developing an index representative of the exploitable pink shrimp population because SEAMAP operates over the areas where the bulk of pink shrimp landings occur (Tortugas fishing grounds). In addition, the FWC survey does not cover the southern estuaries in the Everglades, which are believed to be the primary contributors of pink shrimp recruits to the offshore Tortugas fishing grounds.

The SEAMAP Groundfish survey is characterized by a 42 ft otter trawl that operates in the summer (typically June-July) and fall (typically October-November) of each year, towing both during the day and night. The time series extends from 1987 to 2022 but was only extended East of statistical grid 10, where the bulk of the pink shrimp population resides, starting in 2008. For this index, the Fall and Summer data starting in 2010 were retained for analysis. Given the diurnal burrowing behavior of pink shrimp, the time of day (day vs. night) was expected to impact catch rates. Time of day was accounted for in the modeling process by including a categorical catchability covariate.

2.2.2 Time Series of Environmental Data

Indices of mean annual temperature and salinity in the main nursery grounds (Florida Bay) were developed by Turley, Ailloud, and Stevens (2023), and used to test the impact of environmental conditions on stock abundance. These indices were constructed based on the timing and regions that are thought to supply the bulk of the commercial catches for pink shrimp to capture the variability and trends of the environmental drivers (salinity and temperature) that are most likely to influence recruitment success and, as a result, exploitable biomass. These indices were input into VAST as habitat covariates to test whether their inclusion helped explain a portion of the year-to-year variability observed in the index of relative abundance. A set of lagged indices (one and two years) were also tested.

2.3 Modeling Approach

2.3.1 Model Description

We used the Vector Autoregressive Spatiotemporal (VAST) model v3.11.0 (Thorson and Barnett 2017) implemented in R v.4.4.0 (R Core Team, 2020) to develop indices of relative abundance for each stock. This spatial-delta generalized linear mixed effects model is defined by two linear predictors : p_1 to calculate encounter probabilities (or zero-inflation probabilities in a count-data model) and p_2 for positive catch rates in numbers of shrimp per tow (or the count-data intensity function in a count-data model) for each observation i at location s_i and time t_i.

$$p_1(i) = \beta_1(t_i) + \omega_1^*(s_i) + \epsilon_1^*(s_i, t_i) + \gamma_1(t_i) + \lambda_1(i)$$

$$p_2(i) = \beta_2(t_i) + \omega_2^*(s_i) + \epsilon_2^*(s_i, t_i) + \gamma_2(t_i) + \lambda_2(i)$$

Where β are the year intercepts for each linear predictor (temporal variation, fixed effect), ω^* are the spatial factors (random effects), ϵ^* are the spatio-temporal factors (random effects), γ represent the impacts of habitat covariates on each linear predictor and λ represent the impacts of catchability covariates on each linear predictor. Linear predictors are then transformed to predict encounter probabilities and positive catch rates. In the case of a conventional delta-model :

$$r_1 = logit^{-1}\big(p_1(i)\big)$$

$$r_2 = a_i * exp\big(p_2(i)\big)$$

where a_i is the effort offset (in minutes fished). For pink shrimp, no effort offset was included since all tows were of equal duration. Then, VAST predicts population density $d(s,t)$ at extrapolation grids across a continuous spatial domain (pre-defined to cover the extent of the surveys) and discrete time intervals (years) from both transformed linear predictors as (in the case of a conventional delta-model):

$$d(s,t) = logit^{-1}\big(\beta_1(t_i) + \omega_1^*(s_i) + \epsilon_1^*(s_i, t_i) + \gamma_1(t_i)\big) * exp\big(\beta_2(t_i) + \omega_2^*(s_i) + \epsilon_2^*(s_i, t_i) + \gamma_2(t_i)\big)$$

and calculates the abundance index $I(t)$ in time t as :

$$I(t) = \sum_{s=1}^{n_s} \big(a(s) * d(s,t)\big)$$

where $a(s)$ is the area associated with knot s. Habitat covariates are processes that affect true underlying densities, they are used in both the fitting process and the prediction process. Catchability covariates are processes that affect sampling but do not reflect underlying densities, their estimated effect is removed when calculating the index. Estimates of "density" for pink shrimp are not directly interpretable on an absolute scale as no meaningful estimate of area swept could be produced for these surveys.

Spatial and spatiotemporal variation are estimated using Gaussian Markov random fields (Thorson 2019a). The spatial correlation matrix is modeled using a Matérn covariance function (Lindgren, Rue, and Lindström 2011). The user can specify a Matérn covariance function that is either isotropic (where correlations decline at the same rate in any direction) or anisotropic

(where the rate at which correlations decline depends upon the direction of movement – common in marine ecosystems, where correlations decline slowly when moving along a depth contour but rapidly when moving perpendicular to the depth contour (Thorson 2019a)). The number of prediction locations (i.e. knots) must be predefined. VAST then distributes the knots spatially using a k-means algorithm that minimizes the average distance between samples and knots. A detailed description of the model can be found in (Thorson 2019b) and in the VAST User Manual (Thorson 2024).

2.3.2 Prediction grid

Before fitting VAST models, we constructed prediction grids for the study species. A 3km x 3km extrapolation grid was constructed to encompass the total area covered by the survey (*Figure 2*).

2.3.3 Modeling Workflow

Model development involved the following steps:

1. *Selecting the optimal number of knots :* a delta-lognormal model with both spatial and spatiotemporal random effects and no habitat or catchability covariates was run using a series of knots from 250 to 1500 knots to determine the optimal number of knots to use while balancing computational speed and spatial resolution. The root mean square error (RMSE) between raw observations and fitted values of the index was used to measure differences between runs and find the number of knots beyond which results appeared to stabilize.

2. *Identifying the optimal distribution model :* Candidate models included :

   – a Poisson-link delta-model (*ObsModel=c(2,1)*) : log-linked linear predictor for encounter probability (i.e., Poisson), and a gamma error distribution for positive catch rates;

   – a Zero-inflated negative binomial model (*ObsModel=c(5,0)*) : 1st linear predictor for logit-linked zero-inflation, 2nd linear predictor for log-linked conditional mean of negative binomial;

   – a Conventional lognormal delta-model (*ObsModel=c(4,0)*) : logit-link for encounter probability and log-link for positive catch rates.

   Standard model selection tools (i.e., AIC, qq plots) were used to identify the best fitting model.

3. *Testing the inclusion of spatial and spatiotemporal random effects :* Using the optimal number of knots and distribution function determined in steps 1. and 2., a series of models were built with increasing complexity with respect to including spatial and spatiotemporal random effects. If the estimated variances of the spatial and spatiotemporal terms were greater than zero, the random effects were retained. Random effects, when present, were included in both linear predictors. AIC was used to select the Matérn covariance functions (anisotropic vs. isotropic).

4. *Selecting catchability covariates :* Using the optimal model determined in step 3., we explored the impact of including the following catchability covariates: time of day (tod).

Catchability covariates were included in both linear predictors. AIC was used to assess model fit.

5. *Selecting habitat covariates :* Using the optimal model determined in step 4., we explored the impact of including the following habitat covariates: indices of mean annual temperature and salinity in the nursery grounds and these same indices lagged by 1 and 2 years. Indices were normalized to a mean of zero and standard deviation of 1 prior to input into the model and set up as spatially explicit annual zero-centered covariates to predict changes in density across space and time (i.e., single value across space within a year but varied from year to year). Habitat covariates were included in both linear predictors. AIC was used to assess model (m) fit. Following (Cao et al. 2017), a pseudo-R^2 metric was calculated to determine the proportion of variance (σ^2) from the null model ($null$; i.e., habitat covariates) that was explained by including habitat variables :

$$pseudo - R^2 = 1 - \frac{\sigma^2_{\omega,m} + \sigma^2_{\epsilon,m}}{\sigma^2_{\omega,null} + \sigma^2_{\epsilon,null}}$$

3. Results

1. *Selecting the optimal number of knots :* The RMSE reached an asymptote around 700 knots (*Figure 3*) and there was very little difference in the estimated index using 700 (runtime : 0.3hrs) vs. 1500 knots (run time : 0hrs) (*Figure 4*). A model with 700 knots was therefore retained for subsequent model building steps.

2. *Identifying the optimal distribution model :* AIC and qqplots indicated that the zero-inflated negative binomial model was preferred (*Figure 5*).

3. *Testing the inclusion of spatial and spatiotemporal random effects :* The marginal standard deviation (MSD) of spatial (ω) random effects were significantly greater than zero and thus included in the final model ($\omega_1 = 1.45$; $\omega_2 = 2.32$). However, the MSD for the spatiotemporal (ϵ) random effects tended to zero so the spatiotemporal terms were excluded from the equations. The model that assumed anisotropic covariance was favored in terms of AIC (*Table 1*, *Figure 6*). Including spatial random effects did alter the index values in certain years but the confidence intervals largely overlapped.

4. *Selecting catchability covariates :* The model with the lowest AIC was the model that included time of day and month as catchability covariates (*Table 2*; *Figure 7*). However, including month brought no considerable improvement in fit and inflated the estimated variance around the index. While the time of day effect was clear (*Figure 9*), the month effects plot did not yield any obvious month effect (*Figure 8*). As such, the preferred model was chosen to be one with only time of day as catchability covariate.

5. *Selecting habitat covariates :* Only one of the habitat covariate runs converged (salinity lag=1). Between the two, the Null model with no habitat covariates was favored in terms of AIC (*Table 3*; *Figure 10*).

The final model included spatial random effects using the anisotropic estimation of correlation (*Figure 11*), and catchability covariate time of day in both the 1st and 2nd linear predictors. *Figure 12* shows the final standardized index plotted against the non-standardized index. The

distribution of quantile residuals did not show any substantial spatial pattern (*Figure 13*). The model fit the data reasonably well (*Figure 14*).

4. Discussion

The standardization process did not have an appreciable impact on the overall trend of the index but did result in slightly larger variance estimates (*Figure 12*).

While many studies point to the relationship between shrimp production and salinity on the nursery grounds (see SEDAR (2024c)), average salinity and temperature in the Florida Bay nursery grounds were not found to have an appreciable impact on the annual variation in shrimp density. It is likely that the relationship between CPUE and environmental conditions is not linear and would be better described using a spline where shrimp production is maximized under certain conditions but hampered under extremes. At the time that this work was conducted, it was not possible in VAST to specify a more complex relationship for the environmental index so that option was not explored.

The final model including spatial random effects and a catchability covariate for time of day in both the 1st and 2nd linear predictors but no habitat covariate is recommended as the index for input into JABBA.

References

Cao, Jie, James T. Thorson, R. Anne Richards, and Yong Chen. 2017. "Spatiotemporal Index Standardization Improves the Stock Assessment of Northern Shrimp in the Gulf of Maine." *Canadian Journal of Fisheries and Aquatic Sciences* 74 (11): 1781–93. *https://doi.org/10.1139/cjfas-2016-0137*.

Lindgren, Finn, Håvard Rue, and Johan Lindström. 2011. "An Explicit Link Between Gaussian Fields and Gaussian Markov Random Fields: The Stochastic Partial Differential Equation Approach." *Journal of the Royal Statistical Society Series B: Statistical Methodology* 73 (4): 423–98. *https://doi.org/10.1111/j.1467-9868.2011.00777.x*.

SEDAR. 2023. "SEAMAP Trawl Shrimp Data and Index Estimation Work Group Report." North Charleston, SC. *https://sedarweb.org/documents/sedar-rd01-seamap-trawl-shrimp-data-and-index-estimation-work-group-report/*.

SEDAR. 2024a. "SEDAR 87 Gulf of Mexico White, Pink, and Brown Shrimp SECTION II: Data Workshop Report." SEDAR. *https://sedarweb.org/documents/sedar-87-gulf-of-mexico-white-pink-and-brown-shrimp-data-workshop-report/*.

SEDAR. 2024b. "SEDAR 87 Gulf of Mexico White, Pink, and Brown Shrimp SECTION II: Data Workshop Report." *https://sedarweb.org/documents/sedar-87-gulf-of-mexico-white-pink-and-brown-shrimp-data-workshop-report/*.

SEDAR. 2024c. "SEDAR 87 Gulf of Mexico White, Pink, and Brown Shrimp SECTION II: Data Workshop Report." *https://sedarweb.org/documents/sedar-87-gulf-of-mexico-white-pink-and-brown-shrimp-data-workshop-report/*.

Thorson, James. 2024. "VAST Manual." *https://github.com/James-Thorson-NOAA/VAST/blob/main/manual/VAST_model_structure.pdf*.

Thorson, James T. 2019a. "Guidance for Decisions Using the Vector Autoregressive Spatio-Temporal (VAST) Package in Stock, Ecosystem, Habitat and Climate Assessments." *Fisheries Research* 210 (February): 143–61. *https://doi.org/10.1016/j.fishres.2018.10.013*.

Thorson, James T. 2019b. "Guidance for Decisions Using the Vector Autoregressive Spatio-Temporal (VAST) Package in Stock, Ecosystem, Habitat and Climate Assessments." *Fisheries Research* 210 (February): 143–61. *https://doi.org/10.1016/j.fishres.2018.10.013*.

Thorson, James T., and Lewis A. K. Barnett. 2017. "Comparing Estimates of Abundance Trends and Distribution Shifts Using Single- and Multispecies Models of Fishes and Biogenic Habitat." Edited by Emory Anderson. *ICES Journal of Marine Science* 74 (5): 1311–21. *https://doi.org/10.1093/icesjms/fsw193*.

Turley, Brendan, Lisa Ailloud, and Molly Stevens. 2023. "Development of Estuarine Environmental Indices for SEDAR 87 Gulf of Mexico White, Pink, and Brown Shrimp Stock Assessment." North Charleston, SC. *https://sedarweb.org/documents/sedar-87-ap-01-development-of-estuarine-environmental-indices-for-sedar-87-gulf-of-mexico-white-pink-and-brown-shrimp-stock-assessment/*.

Williams, Jo, Kimberly Johnson, Kyle Detloff, and Alan Lowther. 2024. “SEDAR 87 Commercial Fishery Landings and Effort Figures for White, Pink, and Brown Shrimp in the US Gulf of Mexico, 1960-2022.” North Charleston, SC. *https://sedarweb.org/documents/sedar-84-dw-16-sedar-84-commercial-fishery-landings-and-effort-figures-for-white-pink-and-brown-shrimp-in-the-us-gulf-of-mexico-1960-2021/*.

Winker, Henning, Felipe Carvalho, and Maia Kapur. 2018. “JABBA: Just Another Bayesian Biomass Assessment.” *Fisheries Research* 204 (August): 275–88. *https://doi.org/10.1016/j.fishres.2018.03.010*.

Tables

Run Description	$\sigma_{\omega 1}$	$\sigma_{\omega 2}$	$\sigma_{\varepsilon 1}$	$\sigma_{\varepsilon 2}$	AIC	ΔAIC
No RE					12,324	782
Spatial RE (iso)	1.35	2.35			11,549	7
Spatial (iso) & spatiotemporal REs	1.26	2.39	-0.19	0	11,553	11
Spatial (aniso) & spatiotemporal REs	1.45	2.32	0.00	0	11,546	4
Spatial RE (aniso)	**1.45**	**2.32**			**11,542**	**0**

Table 1. Marginal standard deviation of spatial (ω) and spatiotemporal (ϵ) terms and AIC across runs with different specifications for the spatial and spatiotemporal random effects and associated Matérn covariance function. The run with the lowest AIC is bolded. *RE: random effects; iso : isotropic Matérn covariance function; aniso: anisotropic Matérn covariance function.*

Run Description	$\sigma_{\omega 1}$	$\sigma_{\omega 2}$	$\sigma_{\varepsilon 1}$	$\sigma_{\varepsilon 2}$	AIC	ΔAIC
Null model	1.45	2.32			11,542	1,319
Null model + month	1.47	2.30			11,533	1,311
Null model + tod	1.39	2.46			10,246	24
Saturated model	**1.60**	**2.52**			**10,223**	**0**

Table 2. Marginal standard deviation of spatial (ω) and spatiotemporal (ϵ) terms and AIC across runs with different specifications for the catchability covariates. The run with the lowest AIC is bolded.

Run Description	$\sigma_{\omega 1}$	$\sigma_{\omega 2}$	$\sigma_{\varepsilon 1}$	$\sigma_{\varepsilon 2}$	pseudoR^2_1	pseudoR^2_2	AIC	ΔAIC
Null model	**1.39**	**2.46**			**0.000**	**0.000**	**10,246**	**0**
Null model + salinity (lag=1)	1.39	2.46			0.006	-0.005	10,249	3

Table 3. Marginal standard deviation of spatial (ω) and spatiotemporal (ϵ) terms and pseudo-R2 showing the proportion of variance from the null model (i.e., the model with no habitat covariates included) that is explained by including habitat covariate(s) in the model. The run with the lowest AIC is bolded.

Figures

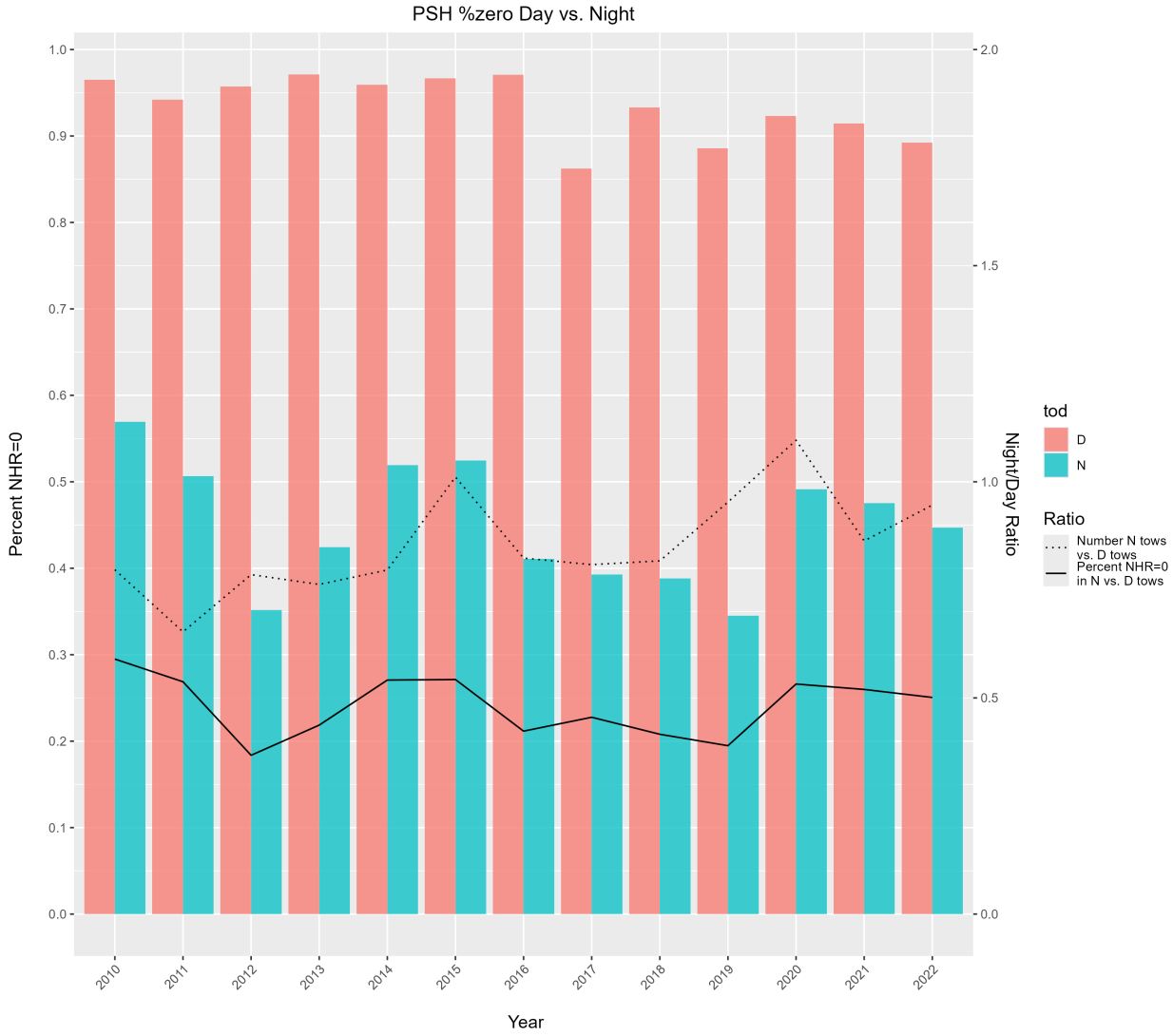

Figure 1: Barplot comparing the fraction (between 0 and 1) of SEAMAP tows with zero catch (NHR = numbers per hour) between daytime (D) and nightime (N) tows (primary y axis). The ratio of zero catch tows during the night vs. day is shown in the black solid line (secondary y axis). The ratio of the number of tows conducted at night vs. during the day is shown in the dashed line (secondary y axis).

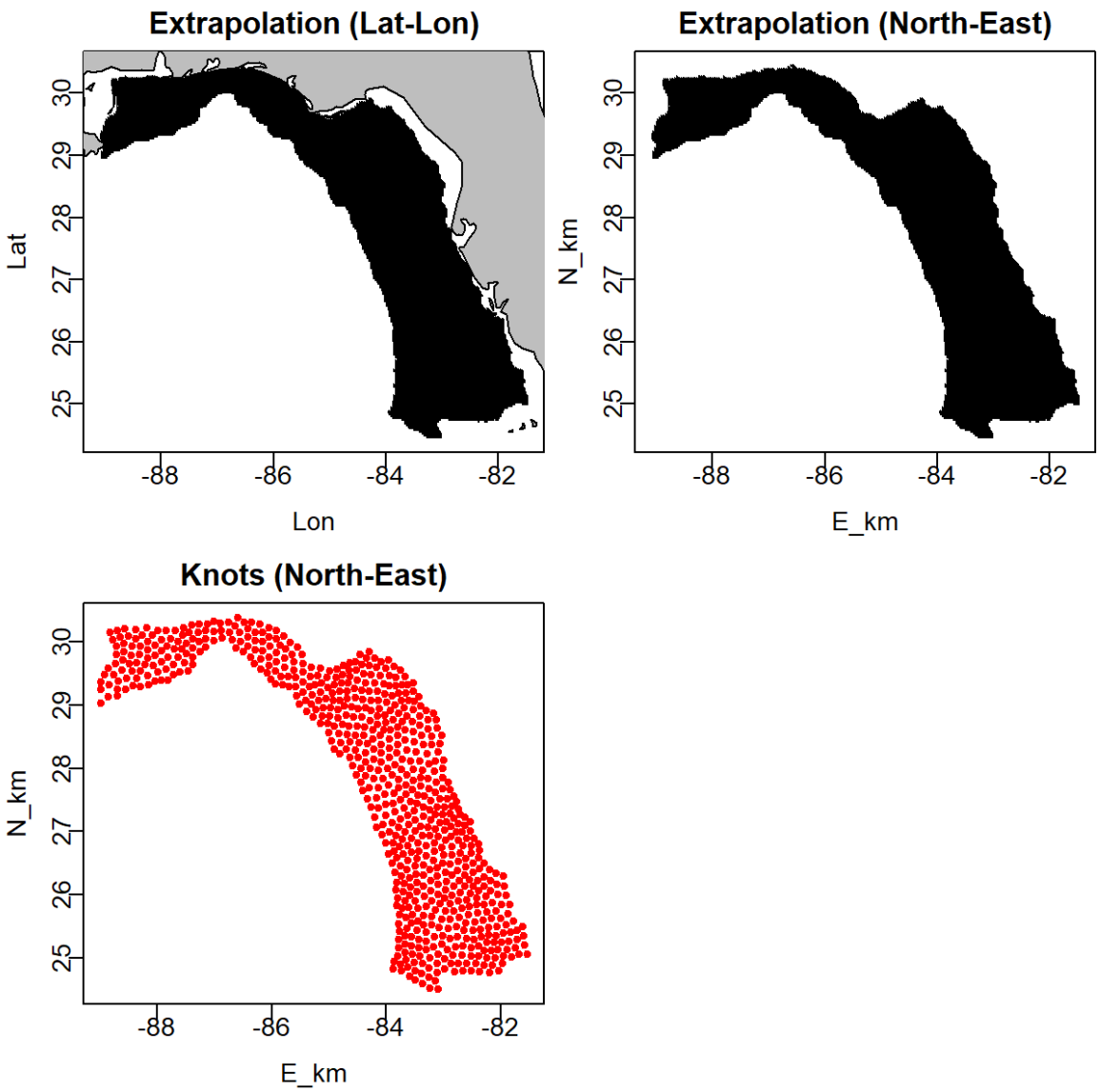

Figure 2: Gulf of Mexico extrapolation region (top panels). For computational efficiency, 700 knots were specified to approximate the spatial and spatiotemporal variation terms of the spatiotemporal model developed in this study (bottom panel).

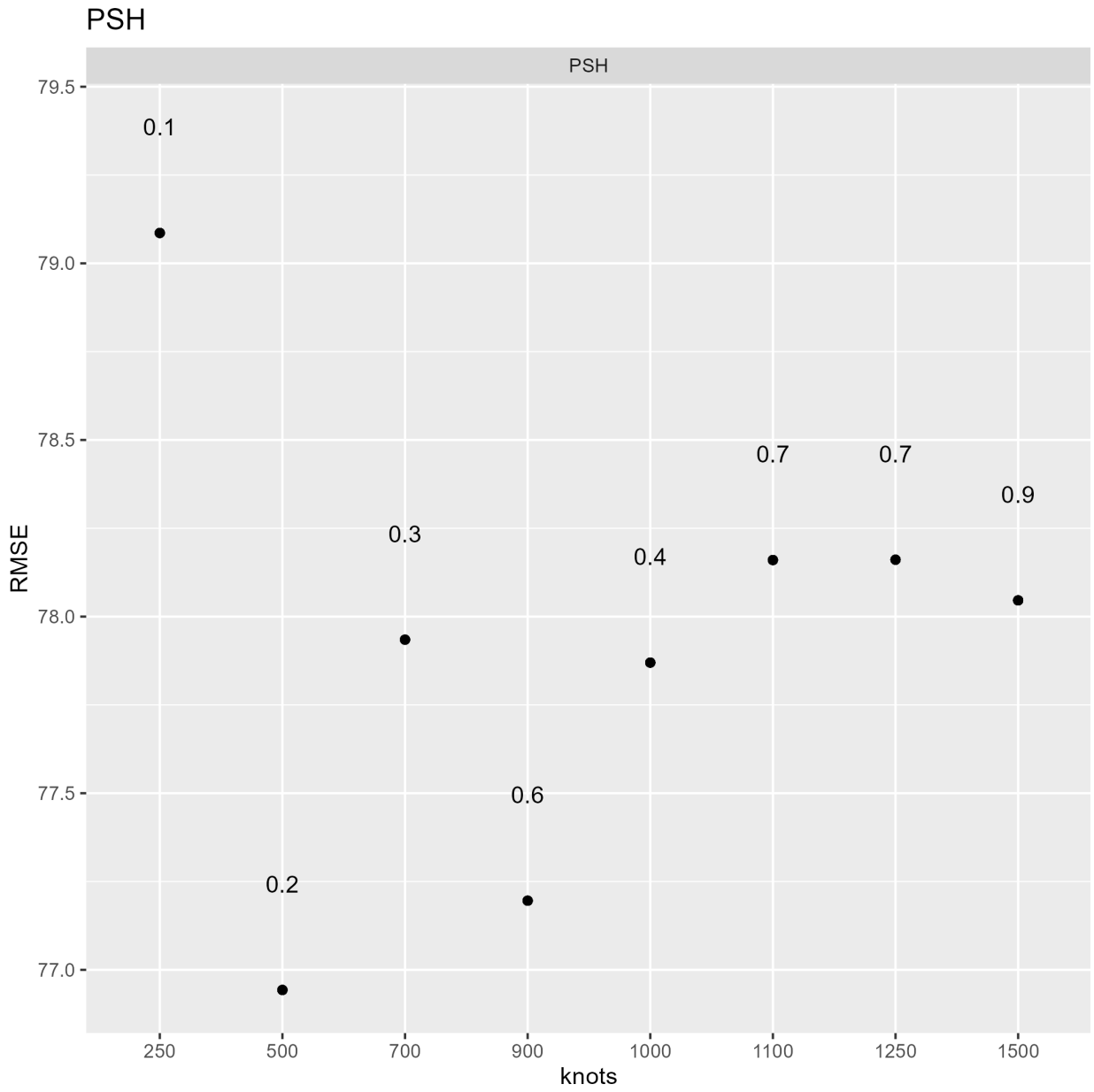

Figure 3: Index RMSE associated with each model run for the different numbers of knots attempted. Run time in hours is printed above each data point. Increasing knot size leads to an asymptote in the RMSE using starting at around 700 knots.

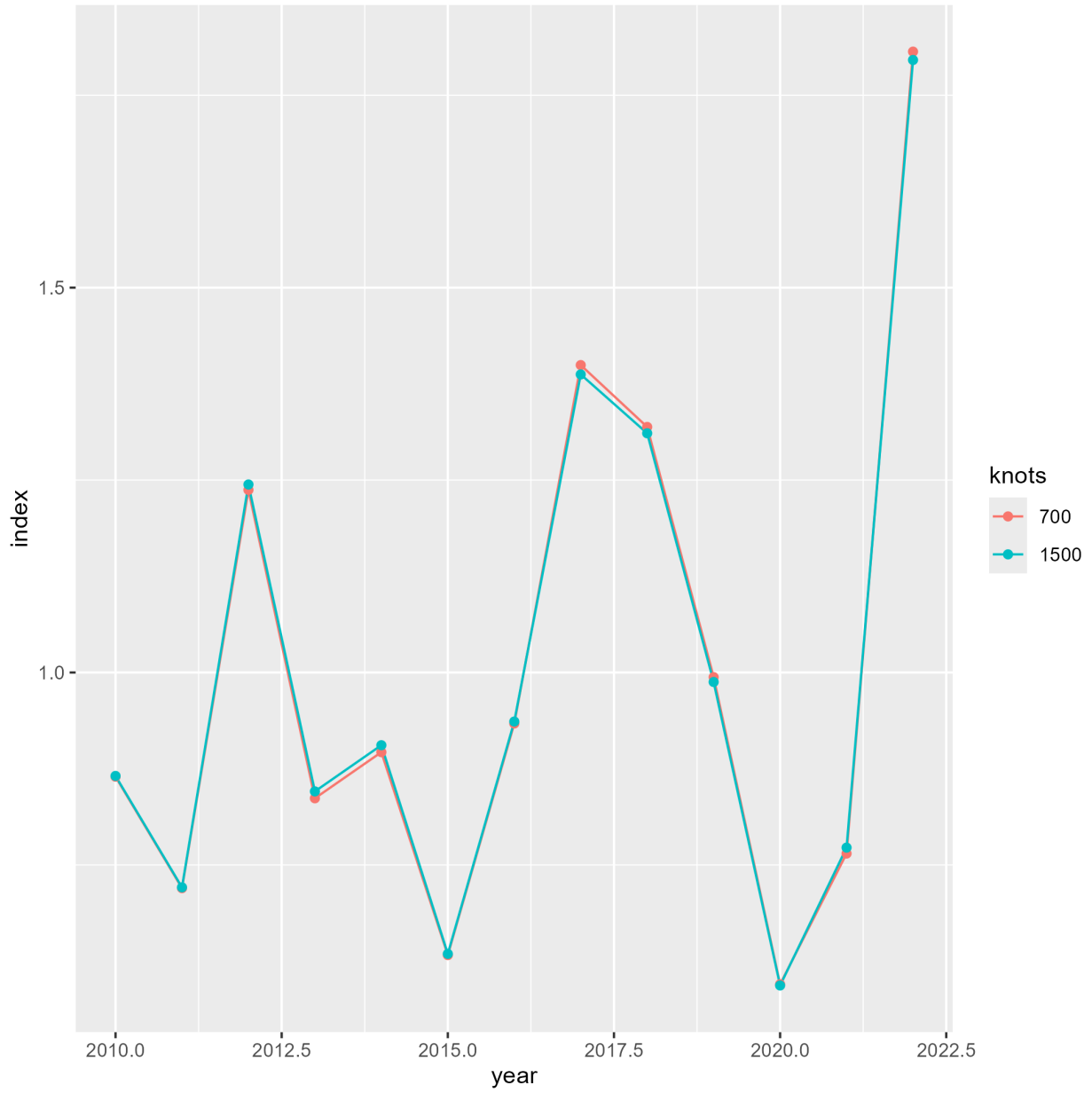

Figure 4: Index estimates for the model run with the highest number of knots (1500) compared with those for the selected model (700).

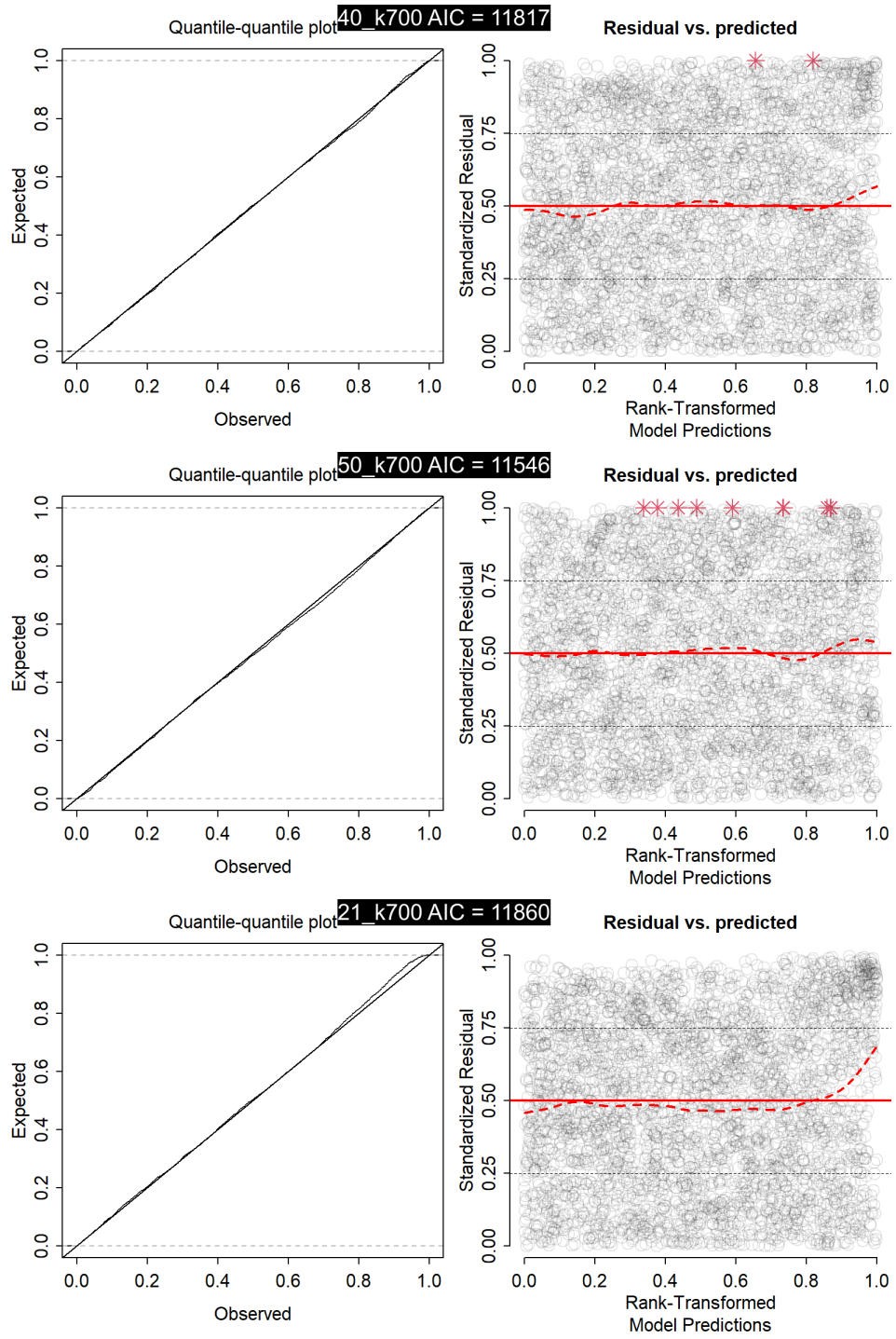

Figure 5: Dharma residual diagnostic plots for the delta-lognormal (top; AIC=11,817), zero-inflated negative binomial (middle; AIC=11,546) and poisson-link (bottom; AIC=11,860) model.

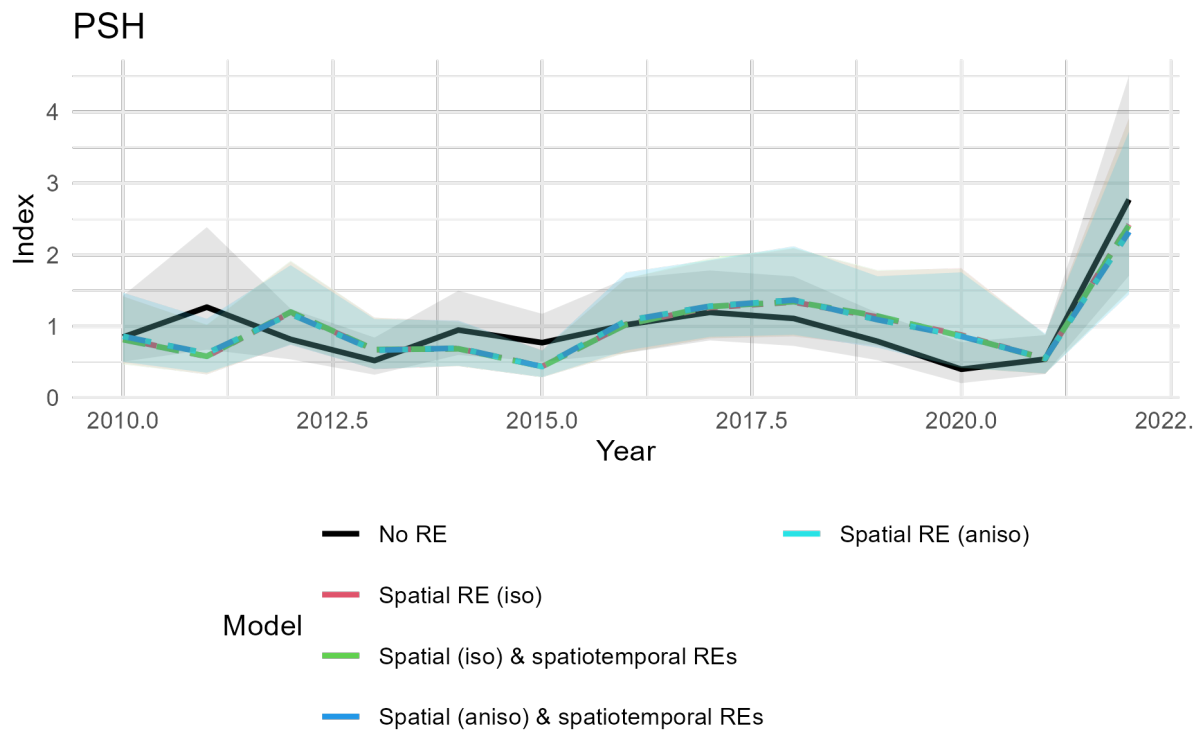

Figure 6: Comparing index estimates and associated confidence intervals across runs with different spatial and spatiotemporal random effects (RE) specifications. iso: isotropic Matérn covariance function; aniso: anisotropic Matérn covariance function.

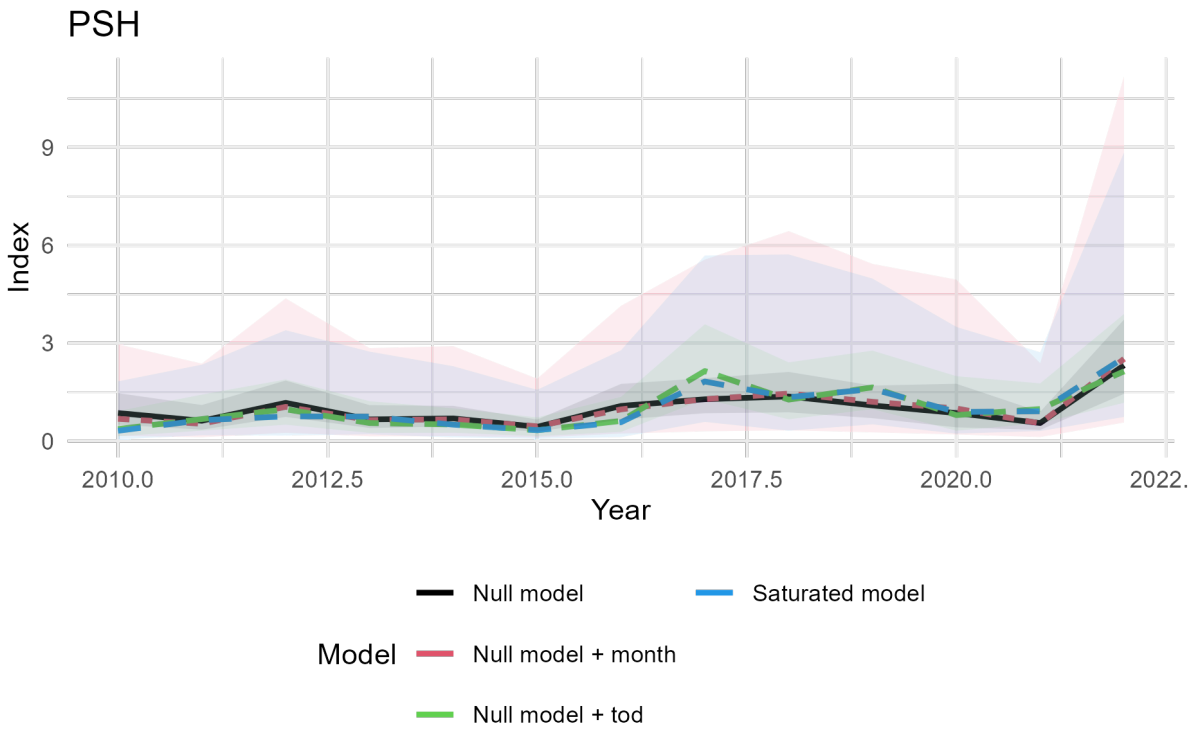

Figure 7: Comparing index estimates and associated confidence intervals across runs with different catchability covariates. The Null model is a model with spatial random effects included in both the 1st and 2nd linear predictors and assuming geometric anisotropy but with no catchability covariates included. tod = time of day (i.e., night vs. day)

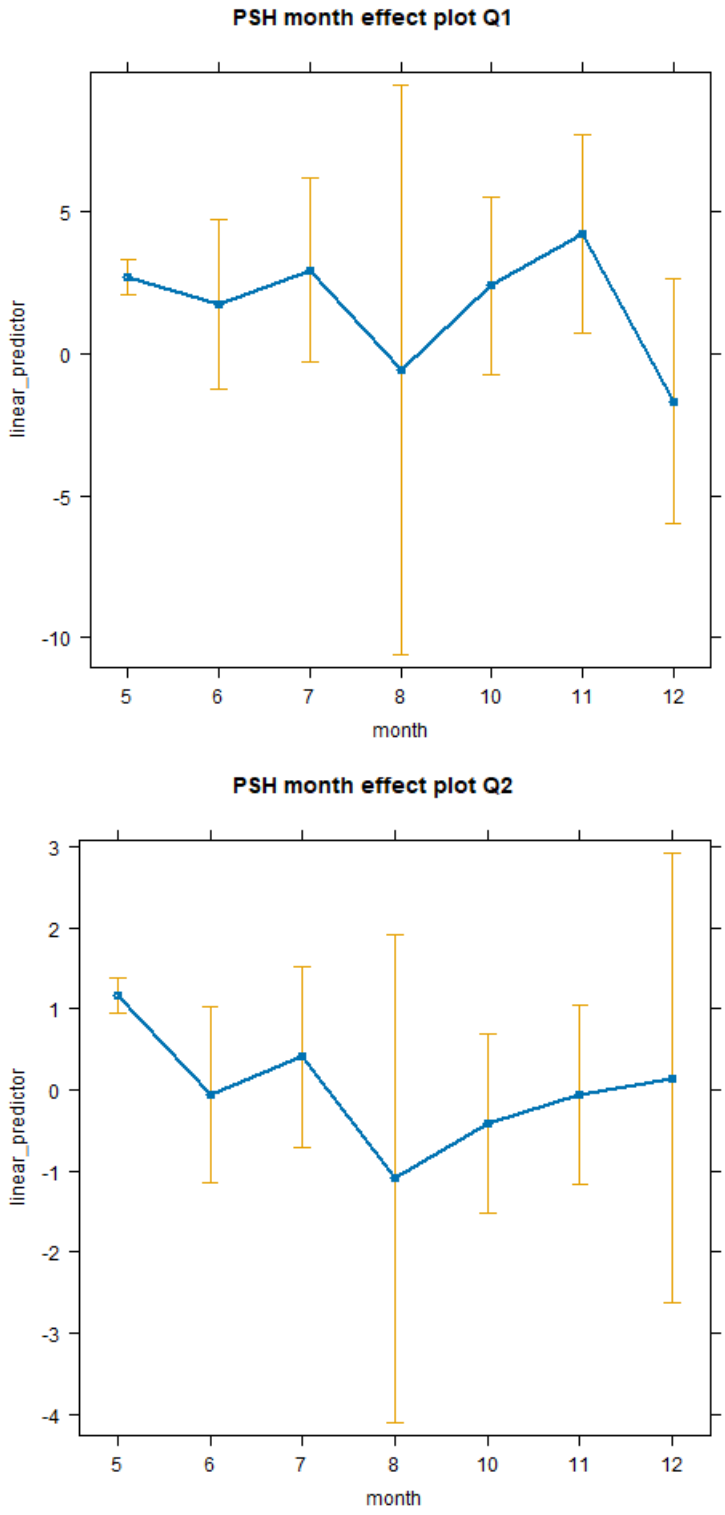

Figure 8: Effect plots for the month catchability covariate. Top panel shows the impact on the first linear predictor, bottom panel shows the impact on the second linear predictor.

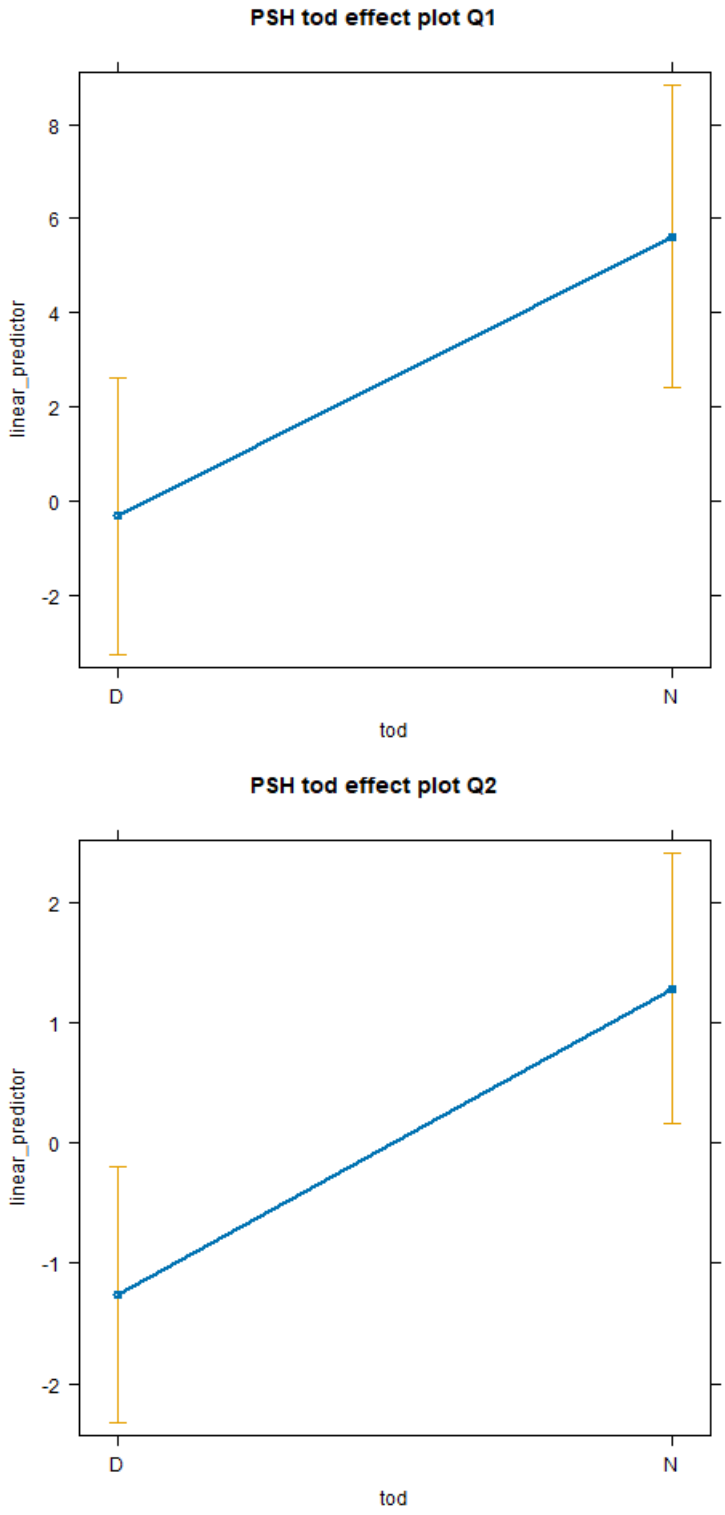

Figure 9: Effect plots for the time of day catchability covariate. Top panel shows the impact on the first linear predictor, bottom panel shows the impact on the second linear predictor.

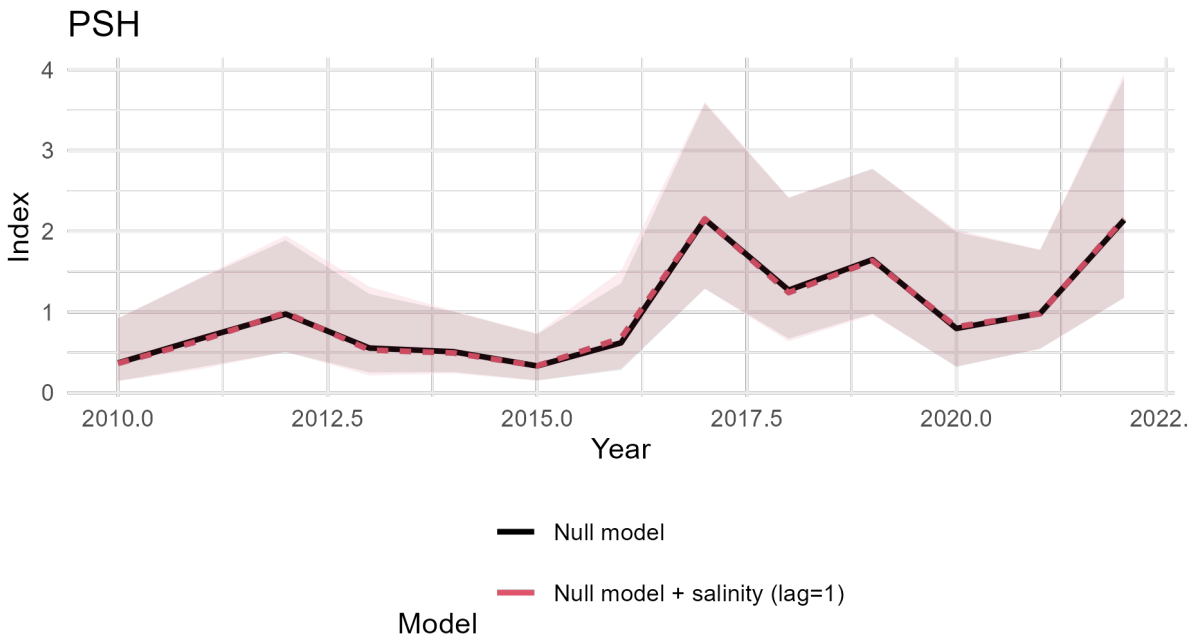

Figure 10: Comparing index estimates and associated confidence intervals across runs with different habitat covariates included. The Null model includes spatial random effects (assuming geometric anisotropy) and a catchability covariate of time of day. temperature = mean annual temperature on the nursery grounds, salinity = mean annual salinity on the nursery grounds, environmental indices are lagged by 0, 1 or 2 years compared with the cpue observations.

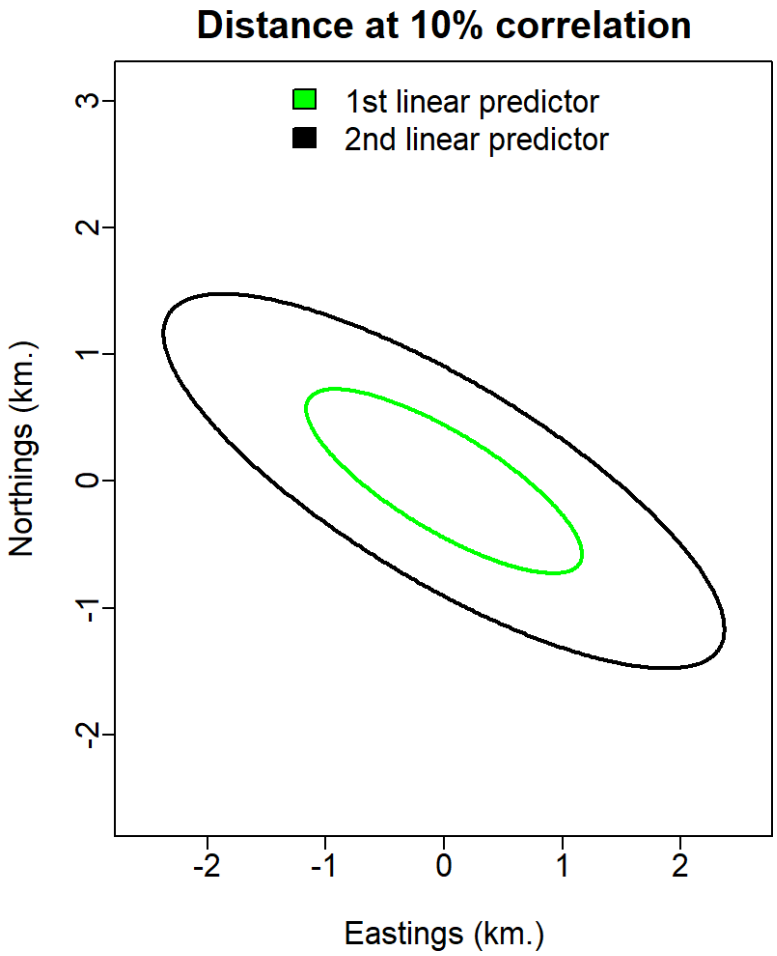

Figure 11: Distance needed to achieve a correlation of approximately 10% from a location centered at coordinates (0,0). Correlations decline slower along the northwest-southeast axis than along the southwest-northeast axis.

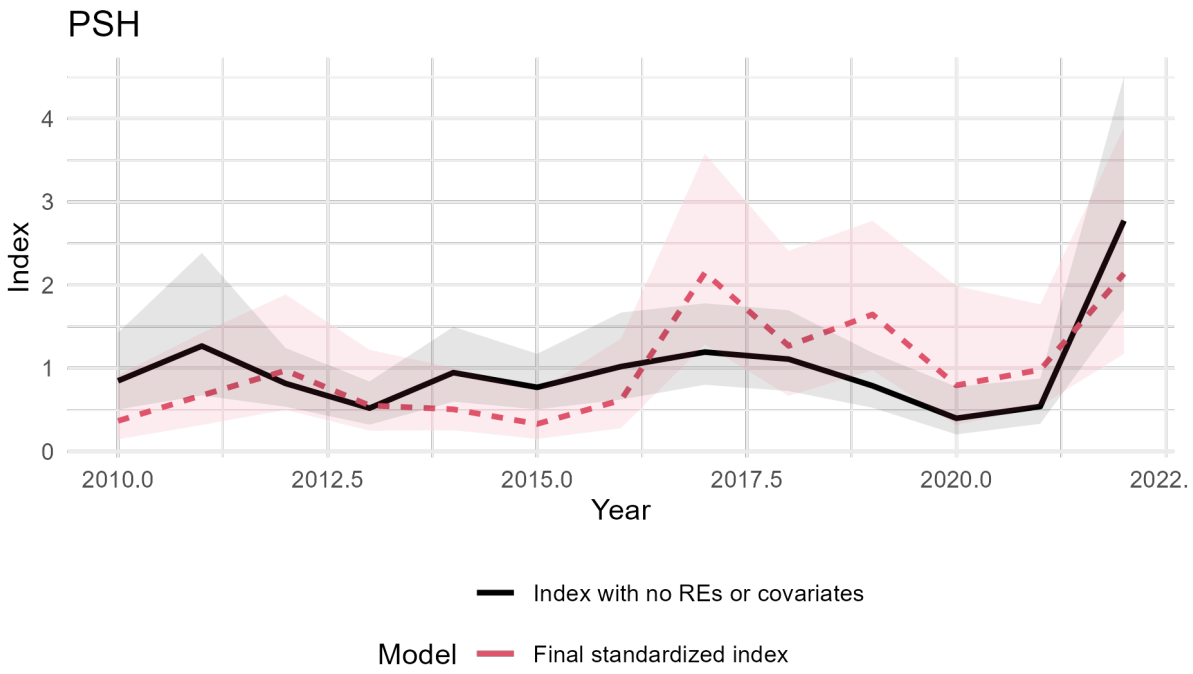

Figure 12: Comparing index estimates and associated confidence intervals for the final model (red) with the preliminary unstandardized index (black). The final index includes a spatial random effect assuming geometric anisotropy and a catchability covariate of time of day.

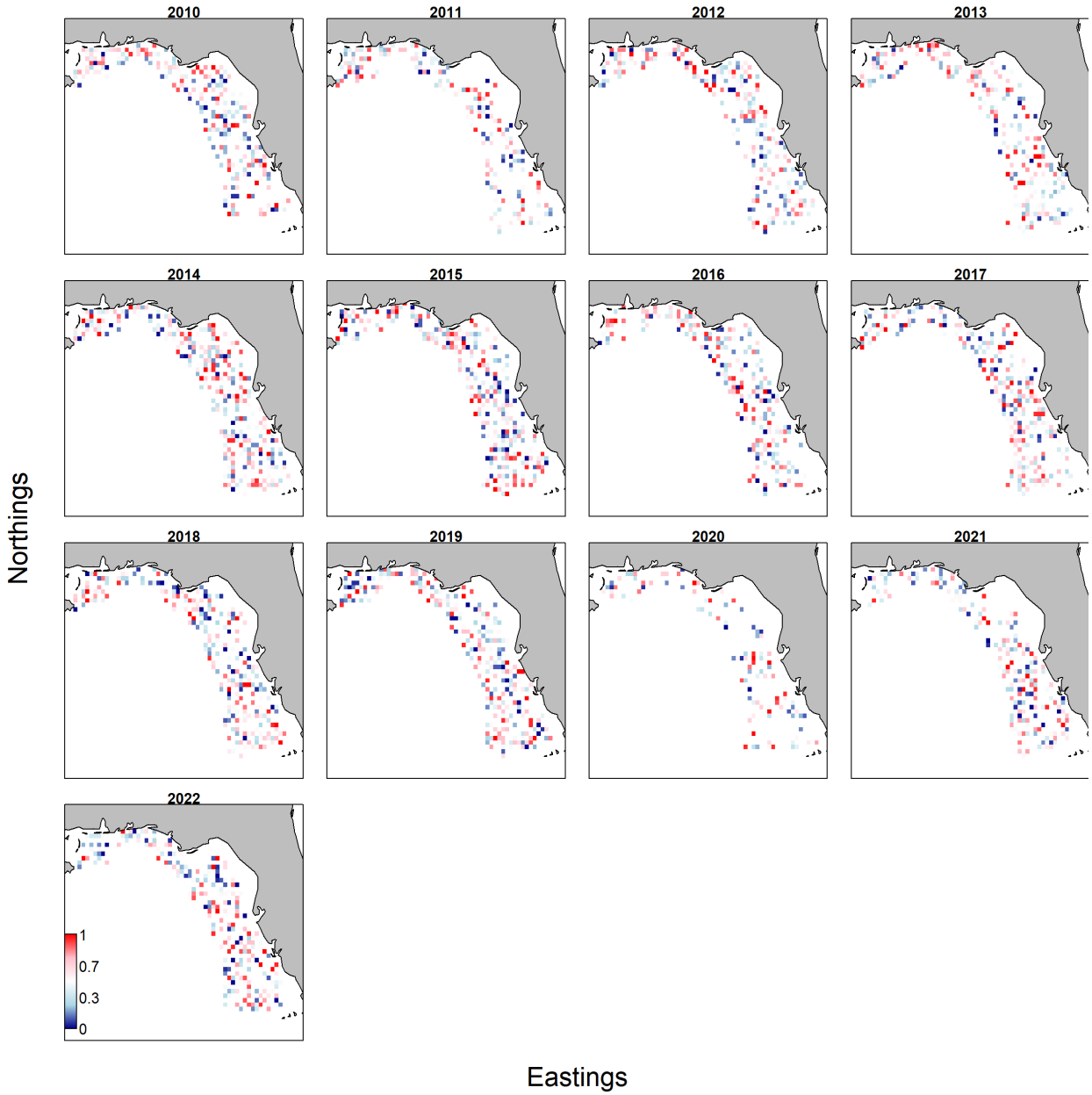

Figure 13: Spatial distribution of quantile residuals for the final model, red color indicating overestimation and blue indicating underestimation.

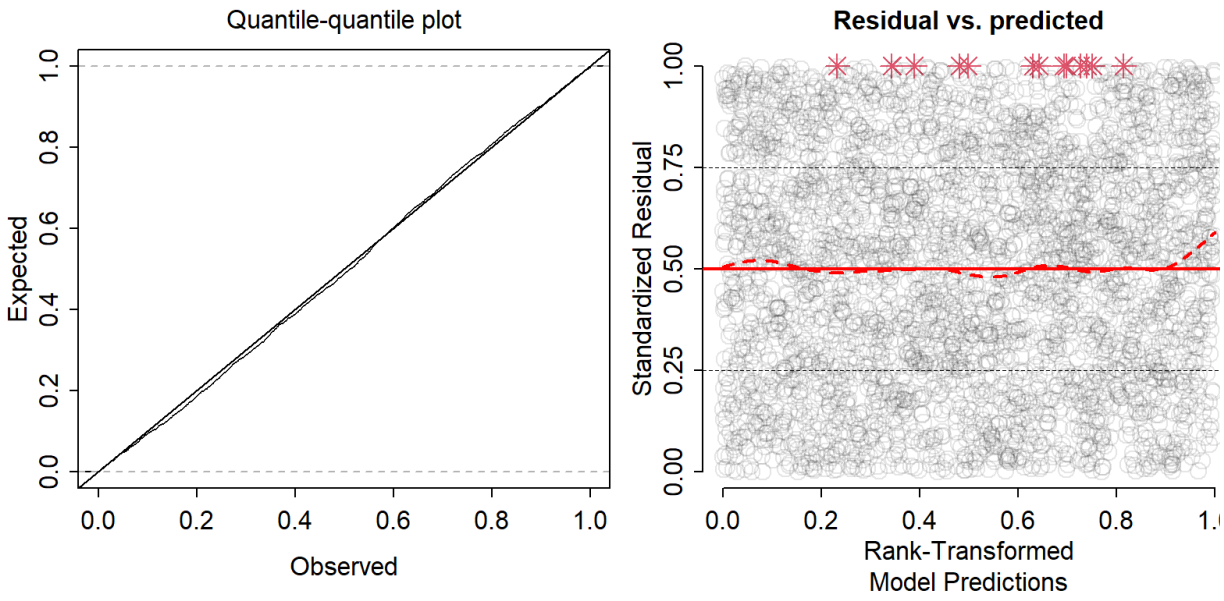

Figure 14: Dharma residual diagnostic plots for the final model.

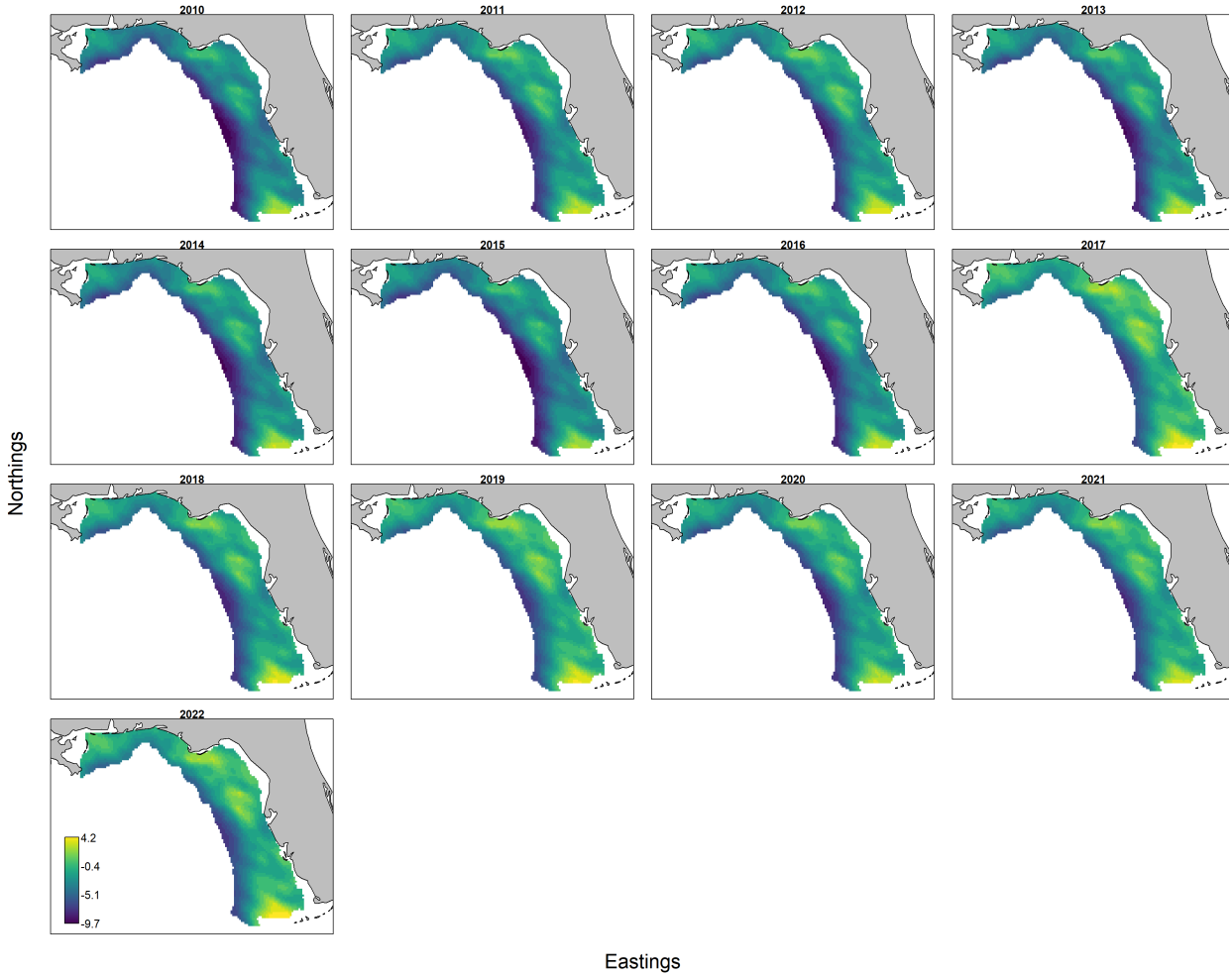

Figure 15: Predicted densities in each year for the final model. The absolute scale is not directly interpretable since no meaningful area swept estimates were available for the development of the index.